Quasioptic dielectric tetrahertz cavity: Coupled through optical tunneling

Weili Zhang, Jiangquan Zhang, and D. Grischkowsky[a)]
School of Electrical and Computer Engineering and Center for Laser and Photonics Research, Oklahoma State University, Stillwater, Oklahoma 74078

(Received 16 November 2000; accepted for publication 26 February 2001)

We report the observation of the well defined oscillation of a picosecond tetrahertz (ps THz) pulse within a dielectric concentric cylindrical cavity, which is coupled to an incoming focused beam of ps THz pulses by the optical tunneling effect of frustrated total internal reflection. The tunneling barrier is an 18-μm-thick air slab, situated between the plane surfaces of a hyperhemicylindrical focusing lens and the cavity. The output of the quasioptic cavity consists of a train of ps THz pulses with a frequency spectrum from 0.1 to 1.0 THz. Good agreement between experiment and theory is obtained in both the time and frequency domains. © *2001 American Institute of Physics.*
[DOI: 10.1063/1.1367901]

The THz frequency range situated between optical and microwave frequencies can utilize either microwave or optical concepts, applications, and combinations. Here, we investigate experimentally and theoretically the periodic oscillation of a freely propagating ps THz pulse injected into a concentric, cylindrical dielectric cavity, which is treated quasioptically in terms of Gaussian beams. For the peak spectral amplitude at 0.5 THz the 5 mm silicon cavity radius is approximately 29 wavelengths in the silicon. This quasioptic situation is in contrast to a previously studied similarly sized, microwave, concentric, cylindrical dielectric cavity with a radius of 7.5 mm and a dielectric constant of 10.8, for which the radius was approximately one-half of the resonant wavelength of 8.04 GHz in the dielectric.[1] In contrast to the direct slot coupling of the microwave case,[1] we employ optical tunneling to couple the quasioptic cavity to an incoming beam of ps THz pulses. Optical tunneling, understood as evanescent coupling, has been widely used in a variety of optical applications such as fiber couplers, laser output couplers, chirp mirrors, and photon tunneling microscopes.[2–4] Compared to the evanescent coupling concepts which give the amplitude coupling, the optical tunneling approach used here gives both amplitude and phase,[8] so that we can calculate the transmission of a well defined short electromagnetic pulse through the tunneling barrier.[5–8]

The cavity system consists of two high-resistivity silicon cylindrical optics, a focusing lens and the cavity itself. An air slab of thickness $d = 18\ \mu$m between the plane surfaces of these two optics is the tunneling coupler for the beam of sub-ps THz pulses incident onto the boundary at an angle beyond critical angle. The output pulses from the cavity come at the repetition rate of 4.39 GHz with a sequential pulse-to-pulse amplitude ratio of 0.7 of the output pulse train. The frequency band of oscillated THz pulses covers the range from 0.1 to 1.0 THz. This THz cavity is theoretically equivalent to an optical concentric microcavity at correspondingly reduced physical size, thereby connecting this work to that involving optical microcavities with dimensions from fifty to hundreds of optical wavelengths.[9–11] Such a well defined short pulse oscillation has not been observed in an optical microcavity.

Because we measure the actual electric field of the circulating THz pulse as a function of cavity roundtrips, we also obtain the corresponding complete spectral characterization (amplitude and phase) of the evolving circulating pulse. This experimental spectral information enables the comparison of our results with that predicted by the recent analytic results for the complex transmission through and the complex reflection from optical tunneling barriers,[8] obtained by the extension of Snell's law to complex angles beyond the critical angle. Our excellent agreement between experiment and theory in both the frequency and time domains reinforces the conclusion of Ref. 8, that the transmission through a tunneling barrier is fully causal and not superluminal, as has been previously considered and claimed.[6,7] In addition, our results demonstrate the feasibility of such THz dielectric cavities and the use of optical tunneling as the high-speed cavity coupler.

The schematic diagram of the experimental setup is presented in Fig. 1(a). The laser system used in this investigation is an argon-laser pumped, self-mode-locked Ti:sapphire laser capable of generating an 800 mW beam of 100 fs optical pulses with central wavelength at 810 nm. Attenuated and split into two arms, the resulting two 7 mW ultrafast laser beams are focused on both the optoelectronic transmitter and receiver in order to generate and detect THz pulses. The bandwidth of this setup covers the range from ~100 GHz to 1.6 THz with a full width at half maximum (FWHM) of 0.6 THz. The THz beam emitted by the transmitter is collimated by the hyperhemispherical silicon lens and the parabolic mirror to a $1/e$ amplitude waist radius of 8 mm at 0.5 THz. A 4-mm-wide slit is inserted into the THz beam path to define the beam entering the cavity. An uncoated pellicle beamsplitter, placed between the slit and the THz cavity, transmits the incoming THz beam to the cavity and reflects the output THz pulse train from the cavity to the receiver. Similar to the standard THz time-domain spectroscopy (THz-TDS) setup,[12] the sample, in this case the cavity, is positioned at the THz beam waist to ensure optimum beam quality at the coupling interface.

[a)]Electronic mail: danielg@thzsun.ecen.okstate.edu

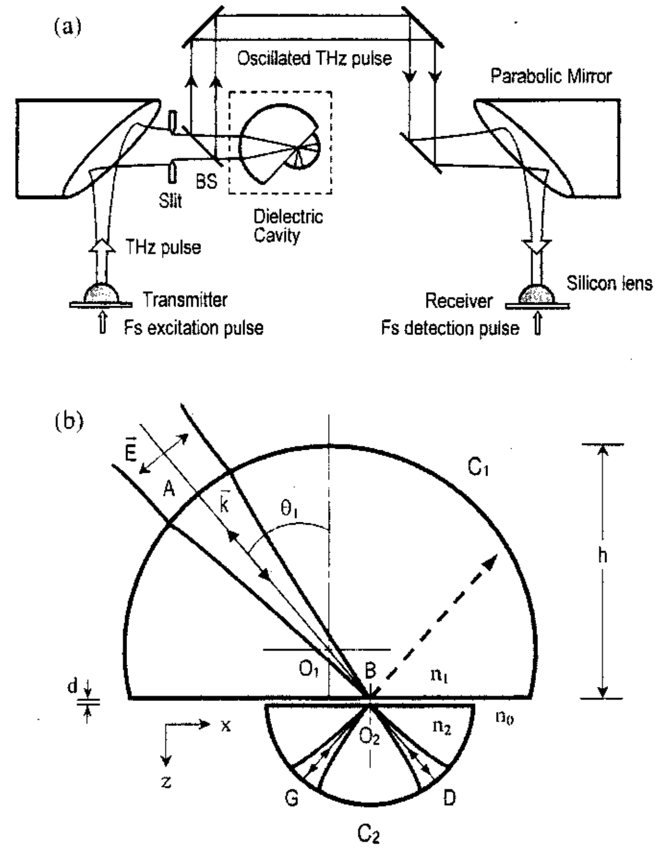

FIG. 1. (a) Schematic diagram of THz cavity layout based on the THz-TDS system. (b) Cross-sectional view of the cylindrical THz cavity system consisting of a hyperhemicylindrical focusing lens C_1 and the quasioptic cavity, the hemicylinder C_2.

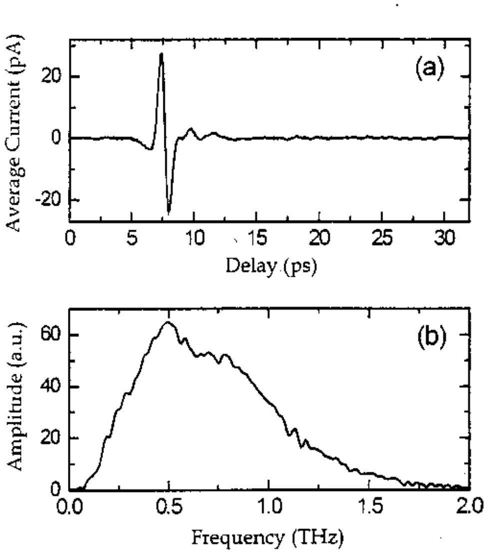

FIG. 2. (a) Measured reference THz pulse and (b) relative amplitude spectrum of the reference pulse.

Consisting of a hyperhemicylindrical focusing lens C_1 and a concentric hemicylindrical cavity C_2, the radial profile of the complete cavity system is shown in Fig. 1(b). Both cylindrical optics are made of high-resistivity silicon, which has nearly negligible absorption and index variation across our THz frequency range.[12] In this setup, $n_1 = n_2 = 3.412$, and $n_0 = 1$. The radii of curvature of the cylindrical optics C_1 and C_2 are 10 and 5 mm, and their centers of curvature are located at O_1 and O_2, respectively; $h = 13$ mm for lens C_1. The lengths of C_1 and C_2 are $l_1 = 20$ mm and $l_2 = 10$ mm, respectively. Thus, when the THz beam is incident from A aligned along a radius into lens C_1 at an angle $\theta_1 = 43.5°$, the focal line is located at B on the flat exit surface of C_1. The cavity C_2 is placed with O_2 coinciding with B on lens C_1 when these two optics are in contact. The resolution for the alignment of rotation and separation between the two plane surfaces of C_1 and C_2 are 0.1° and 1 μm, respectively. Translating C_2 along the direction normal to its plane surface, a homogeneous air gap (the tunneling barrier), sandwiched between two denser media, is formed.

In our cavity, the THz pulses enter the air interface from focal area B at the angle $\theta_1 = 43.5°$ which is much greater than the critical angle $\theta_c = 17.04°$. The transmitted beam of THz pulses is coupled through the air slab into the cavity C_2 by optical tunneling, while the beam reflected by the air slab goes in the direction indicated by the dashed line.

As shown in Fig. 1(b), the incoupled THz pulse oscillates in the hemicylinder C_2 that acts as a concentric cavity,[13–15] in which D and G are the end mirrors connected by the partially reflecting air interface, which is also the output coupler. The THz pulses oscillating in cavity C_2 are P polarized with the electric vector lying in the plane of incidence. The cylindrical surface of cavity C_2 is coated with an aluminum layer with the reflectivity of ~100% for THz radiation. Completely reflected by D, the oscillating pulse is divided into two pulses by the air slab. The pulse transmitted through the air slab is designated as cavity pulse number 1 and propagates along BA, opposite the incident path. The pulse reflected by the air slab at O_2 propagates a roundtrip in the cavity along the track of $O_2G \rightarrow GO_2D \rightarrow DO_2$ and then is partly coupled out by the air slab to be the cavity pulse number 2. The reflected pulse keeps oscillating in the cavity, repeating the above-mentioned track, so that an output cavity THz pulse train with the pulse repetition rate of 4.39 GHz is generated. It is noted that a similar pulse train is emitted in the direction of the dashed line but is trapped in C_1.

The reference THz pulse E_0 is obtained by reducing the thickness of the air slab to zero, $d = 0$. Figures 2(a) and 2(b) illustrate this reference pulse and the corresponding amplitude spectrum. The individual THz pulses of the cavity pulse train are shown as the open circles in Fig. 3(a). The cavity pulses are separated by 228 ps, corresponding to the pulse repetition rate of 4.39 GHz. The average pulse–pulse amplitude attenuation arising from the action of the optical tunneling is ~30% corresponding to the $1/e$, amplitude cavity life time of 0.65 ns. No apparent pulse broadening, due to propagating through the minimally dispersive silicon medium in the cavity is observed. The amplitude spectra of the cavity THz pulses are obtained from a numerical Fourier transform of the time domain data and are shown as open circles in Fig. 3(b). Comparing the amplitude spectra of cavity pulse 1 to pulse 5, there is an obvious attenuation of low frequency components due to the multiple reflections of the pulses by the air slab, whose frequency dependent complex reflectivity is shown in Fig. 4.

We now compare these experimental results with those calculated by linear dispersion theory, where d is the only adjustable parameter. Given the frequency dependent com-

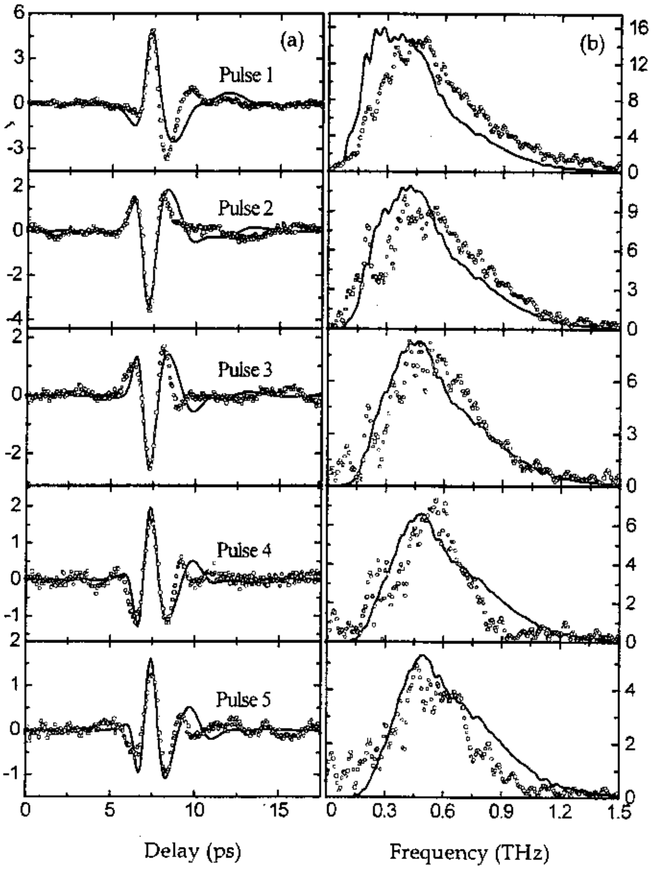

FIG. 3. (a) Measured individual THz pulses (open circles) of the cavity pulse train. The amplitude is in average current (pA); (b) amplitude spectra (open circles) of the measured THz pulses. The solid lines show the corresponding theoretical predictions. These results are normalized with respect to the reference pulse of Fig. 2.

plex amplitude $E_0(\omega)$ of the reference THz pulse and assuming the same path in the cavity for all the frequency components, the complex fields of the cavity pulses $E_j(\omega)$ are determined by

$$E_1(\omega)=t_{ot}^2E_0(\omega), \quad E_{j+1}(\omega)=r_{ot}^2r_{al}^2E_j(\omega), \tag{1}$$

where $j=1, 2, 3, \ldots$ and $t_{ot}=t_{10}t_{02}e^{i\beta}/(1+r_{10}r_{02}e^{2i\beta})$, and $r_{ot}=(r_{10}+r_{02}e^{2i\beta})/(1+r_{10}r_{02}e^{2i\beta})$, are the transmission and reflection coefficients, respectively, of the optical tunneling;[8,16] t_{10}, t_{02}, r_{10}, and r_{02} are the Fresnel coefficients (see Eqs. 1.6.55–58 of Ref. 16) for the transmission and reflection at the boundaries of n_1-n_0 and n_0-n_2, respectively. $\beta=n_0k_0d\cos\theta_0$ is the phase delay associated with multiple reflections inside the air slab, with k_0 the wave vector in free space. θ_0 is the complex refractive angle at the air interface, which is still determined from Snell's law, $n_0\sin\theta_0=n_1\sin\theta_1$, even though the incidence angle θ_1 is beyond the critical angle.[8] $r_{al}=-1$ is the reflection coefficient of the aluminum coating on the cavity C_2. The complex transmission t_{ot} and reflection r_{ot} coefficients of the tunneling for the 18-μm-thick air slab are plotted in Fig. 4, which is similar to the $H(\omega)$ function of Ref. 8. Comparison of the calculated amplitude spectra with that of the measured cavity THz pulses in Fig. 3(b) indicates good agreement with theory for all pulses, and thereby has provided a relatively stringent test of t_{ot} and especially r_{ot} due to the multiple reflections. The calculated cavity pulses are given by the inverse Fourier transform of the calculated complex amplitude spectra $E_j(\omega)$ and as shown in Fig. 3(a) compare favorably with the experimental results.

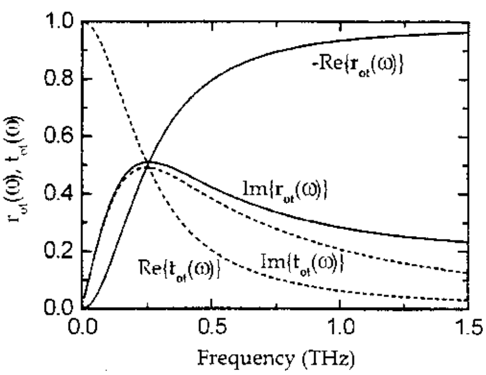

FIG. 4. Calculated complex transmission (dashed lines) and reflection (solid lines) coefficients of the 18-μm-thick air slab.

In conclusion we have shown experimentally and theoretically that the quasioptic oscillation of a ps THz pulse injected into a cylindrical concentric dielectric cavity maintains a well-defined short pulse identity for more than five cavity roundtrips. The evolving cavity pulse shapes are determined by the complex transmission and reflection coefficients of the optical tunneling gap used to couple into and out of the cavity. The excellent agreement between theory and experiment verifies the recently obtained understanding of the causal transmission of a short electromagnetic pulse through an optical tunneling barrier.[8]

The authors acknowledge stimulating discussions with M. T. Reiten, R. A. Cheville, and J. O'Hara. This work was partially supported by the National Science Foundation and the Army Research Office.

[1] R. K. Mongia, A. Ittipiboon, Y. M. M. Antar, P. Bhartia, and M. Cuhaci, IEEE Microwave Guid. Wave Lett. **3**, 38 (1993).
[2] P. Leurgans and A. F. Turner, J. Opt. Soc. Am. **37**, 983 (1947).
[3] J. N. Court and F. K. von Willisen, Appl. Opt. **3**, 719 (1964).
[4] N. S. Kapany and J. J. Burke, *Optical Waveguides* (Academic, New York, 1972).
[5] A. K. Ghatak, M. R. Shenoy, I. C. Goyal, and K. Thyagarajan, Opt. Commun. **56**, 313 (1986).
[6] Ph. Balcou and L. Dutriaux, Phys. Rev. Lett. **78**, 851 (1997).
[7] J. J. Carey, J. Zawadzka, D. A. Jaroszynski, and K. Wynne, Phys. Rev. Lett. **84**, 1431 (2000).
[8] M. T. Reiten, D. Grischkowsky, and R. A. Cheville (unpublished).
[9] A. Ashkin and J. M. Dziedzic, Phys. Rev. Lett. **38**, 1351 (1977).
[10] V. B. Braginsky, M. L. Gorodetsky, and V. S. Ilchenko, Phys. Lett. A **137**, 393 (1989).
[11] L. Collot, V. Lefe'vre-Seguin, M. Brune, J.-M. Raimond, and S. Haroche, Europhys. Lett. **23**, 327 (1993).
[12] D. Grischkowsky, S. Keiding, M. van Exter, and Ch. Fattinger, J. Opt. Soc. Am. B 7, 2006 (1990).
[13] H. Kogelnik and T. Li, Appl. Opt. **5**, 1550 (1966).
[14] C. W. Erickson, IEEE Trans. Microwave Theory Tech. **MTT-23**, 218 (1975).
[15] B. E. A. Saleh and M. C. Teich, *Fundamentals of Photonics* (Wiley, New York, 1991).
[16] M. Born and E. Wolf, *Principles of Optics* (Cambridge University Press, New York, 1999).